BIOMOLECULES & THERAPEUTICS

Original Article
Biomol Ther 31(1), 82-88 (2023)

Functional Characterization of *Drosophila melanogaster* CYP6A8 Fatty Acid Hydroxylase

Sang-A Lee[1], Vitchan Kim[1], Byoungyun Choi[1], Hyein Lee[2], Young-Jin Chun[2], Kyoung Sang Cho[1] and Donghak Kim[1,*]

[1]Department of Biological Sciences, Konkuk University, Seoul 05025,
[2]College of Pharmacy, Chung Ang University, Seoul 06974, Republic of Korea

Abstract

Genomic analysis indicated that the genome of *Drosophila melanogaster* contains more than 80 cytochrome P450 genes. To date, the enzymatic activity of these P450s has not been extensively studied. Here, the biochemical properties of CYP6A8 were characterized. *CYP6A8* was cloned into the pCW vector, and its recombinant enzyme was expressed in *Escherichia coli* and purified using Ni^{2+}-nitrilotriacetate affinity chromatography. Its expression level was approximately 130 nmol per liter of culture. Purified CYP6A8 exhibited a low-spin state in the absolute spectra of the ferric forms. Binding titration analysis indicated that lauric acid and capric acid produced type I spectral changes, with K_d values 28 ± 4 and 144 ± 20 μM, respectively. Ultra-performance liquid chromatography–mass spectrometry analysis showed that the oxidation reaction of lauric acid produced (ω-1)-hydroxylated lauric acid as a major product and ω-hydroxy-lauric acid as a minor product. Steady-state kinetic analysis of lauric acid hydroxylation yielded a k_{cat} value of 0.038 ± 0.002 min^{-1} and a K_m value of 10 ± 2 μM. In addition, capric acid hydroxylation of CYP6A8 yielded kinetic parameters with a k_{cat} value of 0.135 ± 0.007 min^{-1} and a K_m value of 21 ± 4 μM. Because of the importance of various lipids as carbon sources, the metabolic analysis of fatty acids using CYP6A8 in this study can provide an understanding of the biochemical roles of P450 enzymes in many insects, including *Drosophila melanogaster*.

Key Words: P450, CYP6A8, *Drosophila melanogaster*, Lauric acid, Capric acid, Mass spectrometry

INTRODUCTION

Cytochrome P450 (P450s, CYPs) constitute a superfamily of heme-thiolate proteins that exhibit a specific absorption spectrum at 450 nm upon binding to carbon monoxide (CO) (Antoun *et al*., 2006). P450 enzymes catalyze the oxidative reactions of various compounds, including exogenous and endogenous chemicals (Guengerich, 2018). P450 enzymes are distributed in various organisms, from bacteria to plants and animals, including insects (Werck-Reichhart and Feyereisen, 2000). In particular, insect P450 enzymes are involved in the synthesis of ecdysteroids and juvenile hormones, as well as in the degradation of foreign insecticidal chemicals of natural or synthetic origin (Feyereisen, 1999). *Drosophila melanogaster* has 90 P450-like sequences, of which 83 appear to be functional P450 genes and seven are probable pseudogenes (Tijet *et al*., 2001). Among the P450s from *D. melanogaster*, CYP306A1, CYP302A1, CYP315A1, and CYP314A1 are involved in the catalytic reactions of ecdysteroids; they convert cholesterol to 20-hydroxyecdysone via carbon 25-hydroxylation, which is an essential enzymatic step in ecdysteroid biosynthesis during insect development (Niwa *et al*., 2004; Pondeville *et al*., 2013). The P450 gene superfamily has diversified into 25 different families within the *D. melanogaster* genome grouped into four large clades, which specialize in copy number expansions that mostly occur within the CYP4 and CYP6 families within the CYP3 clade (Seong *et al*., 2018). The CYP6A family in *D. melanogaster* has two major physiological roles, insecticide resistance and pheromone synthesis. Baculovirus-directed production of CYP6A2 induced the metabolism of cyclodiene, organophosphorus insecticides, and dichlorodiphenyltrichloroethane (DDT) (Dunkov *et al*., 1997; Amichot *et al*., 2004). The other function of CYP6 family enzymes is the regulation of pheromones to influence behavior patterns. CYP6A20 is expressed in non-neuronal support cells related to pheromone-sensing olfactory sensilla, indicat-

Open Access **https://doi.org/10.4062/biomolther.2022.084**

Received Jun 20, 2022 **Revised** Jul 15, 2022 **Accepted** Jul 20, 2022
Published Online Aug 8, 2022

***Corresponding Author**
E-mail: donghak@konkuk.ac.kr
Tel: +82-2-450-3366, Fax: +82-2-3436-5432

ing that social experience may influence aggressiveness by regulating pheromone sensitivity (Wang *et al*., 2008).

In the CYP6A family, *cyp6a8* is located on the right arm of chromosome 2 and is clustered with other *cyp6a* families and *cyp317a1*. The amino acid sequence of CYP6A8 has 53.6% identity with that of CYP6A2, and both enzymes are overexpressed in DDT-resistant 91-R *D. melanogaster* strains (Maitra *et al*., 1996). The tissue expression level of CYP6A8 has been found to be high in the fly Malpighian tubules. Since the Malpighian tubules are the main organ responsible for detoxification, CYP6A8 has been speculated to play an important role in the detoxification of exogenous substances.

Here, we cloned CYP6A8 from *Drosophila melanogaster*, expressed the recombinant enzyme in *Escherichia coli*, and purified it. The purified CYP6A8 protein was characterized by spectroscopic and enzymatic analyses using various fatty acids.

MATERIALS AND METHODS

Chemicals

Lauric acid, capric acid, glucose-6-phosphate, glucose-6-phosphate dehydrogenase, dilauroyl-L-phosphatidylcholine (DLPC), imidazole, and $NADP^+$ were purchased from Sigma-Aldrich (St. Louis, MO, USA). Ni^{2+}-nitrilotriacetate (NTA) agarose was purchased from Thermo Fisher Scientific (Waltham, MA, USA). 3-[(3-Cholamidopropyl) dimethylammonio]-1-propanesulfonate (CHAPS) was purchased from GoldBio (St. Louis, MO, USA). Rat NADPH-P450 reductase (NPR) was heterologously expressed in *E. coli* HMS174 (DE3) cells and purified as described previously (Park *et al*., 2017). All the other chemicals used were of the highest commercially available grade.

Construction of CYP6A8 expression plasmids

The cDNA of the *D. melanogaster* P450 6A8 gene was provided by the Drosophila Genomics Resource Center (DGRC, Bloomington, IN, USA). The open reading frame (ORF) regions of P450 6A8 were amplified using polymerase chain reaction (PCR) using the following primers with NdeI and XbaI restriction sites and 6×Histidine-tag at the C-terminus: 5′-GCCCGGCCATATGTGCGTTGACTTACATC-3′ and 5′-CTGAAGGTGGAGACCGTCCATCATCATCATCATCATTAATCTAGAGCC-3′. The 1.5 kb amplified PCR fragment was purified using agarose gel electrophoresis and cloned into the pCW expression vector. The constructed vector clones were confirmed using nucleotide sequencing analysis.

Expression and purification of recombinant enzymes

CYP6A8 was expressed and purified as previously described, with some modifications (Park *et al*., 2017). The *E. coli* strain was transformed with a pCW expression vector and plated on Luria-Bertani (LB) medium containing 50 μg/mL ampicillin. Individual colonies were inoculated in LB broth containing 50 μg/mL ampicillin and incubated overnight in a shaking incubator at 37°C and 230 rpm. The LB liquid cultures were transferred into 500 mL of Terrific broth (TB) (Thermo Fisher Scientific) containing 50 μg/mL ampicillin and incubated at 37°C and 230 rpm until the optimal density at 600 nm was 0.5. Protein expression was performed by adding supplements (0.5 mM delta-aminolevulinic acid, 1 mM isopropyl β-D-1-thiogalactopyranoside (IPTG), 1 mM thiamine, and trace elements). The expression cultures were incubated at 28°C and 200 rpm for 44 h and harvested by centrifugation at 4000 rpm for 30 min. The harvested cells were resuspended in TES buffer [100 mM Tris-acetate, 0.5 mM EDTA, and 500 mM sucrose] containing lysozyme, incubated at 4°C for 30 min, centrifuged at 4000 rpm for 30 min, and sonicated with sonication buffer [0.1 mM dithiothreitol and 100 mM phenyl-methylsulfonyl fluoride]. The sonicated fraction was centrifuged at 5,000×*g* for 20 min, and the supernatant was ultracentrifuged at 65,100×*g* for 2 h. The prepared membrane fraction was solubilized overnight in a solubilization buffer containing 1 mM EDTA, 10 mM β-mercaptoethanol, and 1% CHAPS (w/v). The solubilized proteins were purified using Ni^{2+}-nitrilotriacetate (NTA) affinity column chromatography. The eluted protein fraction was subsequently dialyzed at 4°C in 100 mM potassium phosphate buffer (pH 7.4) containing 20% glycerol and 0.1 mM EDTA.

Spectroscopic characterization and spectral binding titration analysis

The purified CYP6A8 enzymes were diluted to 1 μM with 100 mM potassium phosphate buffer (pH 7.6) and split into two spectroscopic glass cuvettes. Spectroscopic changes (350-500 nm) were measured upon the addition of ligands using a CARY 100 Varian spectrophotometer (Agilent Technologies, CA. USA). Binding spectral titration with fatty acids was examined. It also worked with azoles. The difference between the maximum and minimum wavelengths in absorbance was plotted against the substrate concentration to calculate the substrate-binding affinities (K_d).

P450 catalytic activity analysis

P450 catalytic activity was determined using purified CYP6A8 enzymes and rat NADPH-P450 reductase (NPR) in reconstituted systems. Hydroxylation of fatty acids was analyzed using ultra-performance liquid chromatography-tandem mass spectrometry (UPLC–MS/MS) (Waters, Milford, MA, USA). The reaction mixture included 0.2 μM CYP6A8, 0.4 μM rat NPR, and 1,2-dilauroyl-*sn*-glycerol-3-phosphocholine (DLPC, 30 μg) in 0.5 mL of 100 mM potassium phosphate buffer (pH 7.4). After 3 min of preincubation at 37°C, an NADPH-generating system [100 mM glucose 6-phosphate, 10 mM $NADP^+$, and glucose-6-phosphate dehydrogenase] was used to initiate the enzymatic reactions. The reaction was conducted for 10 min at 37°C and terminated by the addition of 1 mL of CH_2Cl_2. The product was extracted by vortex mixing and centrifugation at 3500 rpm for 15 min. The organic (lower) layer was transferred to a clean test tube and dried under N_2 gas. The dried products were dissolved in 100 μL of methanol and transferred to a glass vial before analysis by UPLC-MS/MS.

These samples were injected into an ACQUITY UPLC™ BEH C18 column (50×2.1 mm, 1.7 μM) equipped with Waters ACQUITY UPLC™ (Waters) and Waters Quattro Premier™ (Waters). For the analysis of lauric acid hydroxylation, the mobile phase consisted of H_2O containing 10% CH_3CN (with 0.05% acetic acid) (A) and 100% CH_3CN (with 0.05% acetic acid) (B), at a flow of 0.3 mL/min. Mobile phase B was initially held at 30% for 0.5 min and then increased to 53% for 4 min, followed by 100% for 5.5 min. For the analysis of capric acid hydroxylation, the mobile phase composition was identical to that of lauric acid at a flow of 0.2 mL/min. Mobile phase B was initially held at 10% for 0.5 min and then increased to 65% for 6 min, followed by 100% for 7.5 min. The analytes were ob-

served using negative electrospray ionization and the selected ion recording (SIR) mode. The capillary voltage was –2.5 kV and the cone voltage was –36 V. The source temperature was 120°C, desolvation temperature was 300°C, desolvation gas flow rate was 400 L/h, and cone gas flow rate was 30 L/h. The column temperature was maintained at 40°C. The negative ionization transitions of lauric acid (m/z 199.3), hydroxylauric acid (m/z 215.3), capric acid (m/z 171.2), and hydroxycapric acid (m/z 197.2) were analyzed.

Molecular docking modeling of CYP6A8

Docking analysis of CYP6A8 with capric and lauric acids was performed using the Autodock 4.2 software (The Scripps Research Institute, La Jolla, CA, USA). Homology structure modeling of CYP6A8 was performed on the basis of the structure of CYP3A4 (PDB ID:5VCD) using SWISS-MODEL (Swiss instrument of Bioformatics, Torsten Schwede, Switzerland). Capric and lauric acid molecules were obtained from the Protein Data Bank (PDB; PDB ids: DKA and DAO) and used for docking. All water molecules, except the prosthetic heme groups, were removed from the PDB prior to docking.

RESULTS

Purification and spectral characterization of P450 6A8

CO-binding different spectral analysis showed that the expression level of CYP6A8 in the *E. coli* whole-cell was approximately 128.6 nmol/L culture (Fig. 1A). Solubilization using CHAPS rendered CYP6A8 protein in the soluble fraction, which was purified using Ni^{2+}-NTA affinity column chromatography. The SDS–polyacrylamide gel electrophoresis of purified protein indicated a single band of 56 kDa in size, corresponding to the expected size of the ORF region of CYP6A8 (Fig. 1B inset). Purified CYP6A8 showed typical CO-binding Soret spectra at 450 nm and little absorption at 420 nm (Fig. 1B). The absolute spectra of the ferric forms indicated a low-spin state with Soret bands at 419 nm and smaller α- and β-bands at 570 nm and 536 nm, respectively (Fig. 1C). The ferrous form of CYP6A8, reduced by sodium dithionite, showed a broad peak at approximately 422 nm and shifts of the α- and β-bands to 558 and 533 nm, respectively.

Binding of fatty acids to CYP6A8

Binding titration analysis of P450 6A8 was performed using various fatty acids. Titration of CYP6A8 with lauric acid displayed

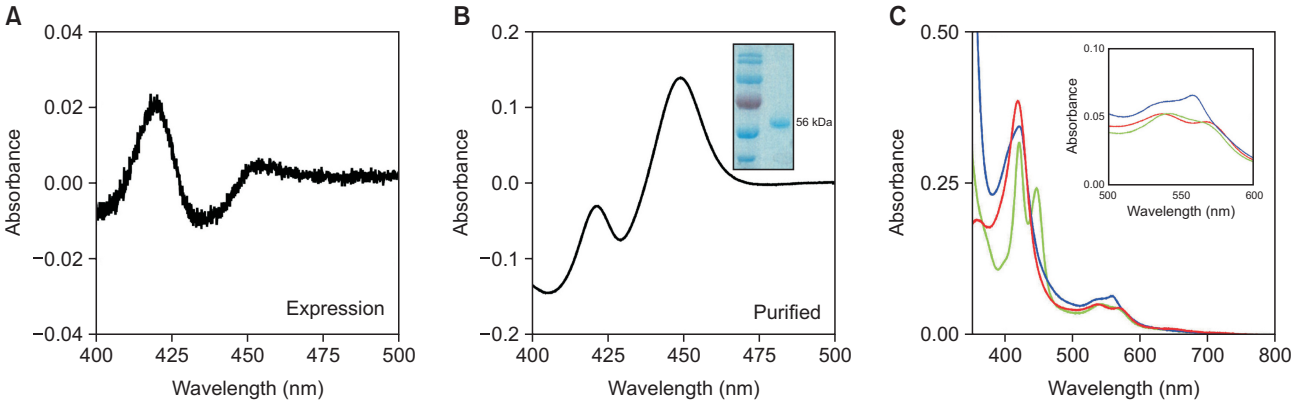

Fig. 1. Expression, purification, and absolute spectra of purified CYP6A8 enzyme. (A) CO-binding differential spectra of CYP6A8 at the *E. coli* whole-cell level. (B) CO-binding differential spectra of purified CYP6A8. (C) Absolute spectra of purified CYP6A8. Absolute spectra of ferric (red), ferrous (blue), and ferrous carbon monoxide protein (green).

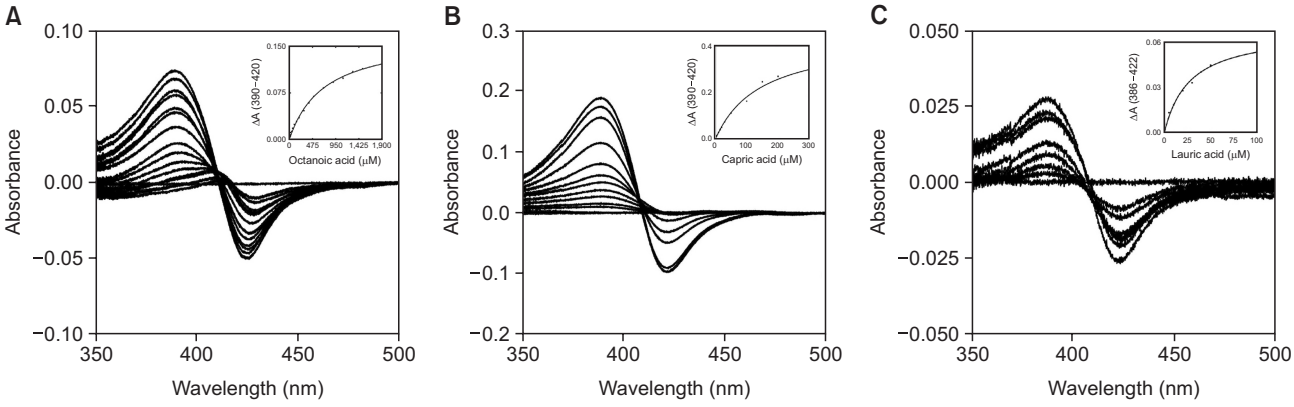

Fig. 2. Binding of octanoic, capric, and lauric acid to CYP6A8 enzyme. Octanoic acid (A), capric acid (B), lauric acid (C) binding titration with purified CYP6A8 enzyme. The insets show the plots of $\Delta(Abs_{max}–Abs_{min})$ vs. the concentration of fatty acids.

typical type-I spectral changes, with an increase at 390 nm and a decrease at 420 nm, indicating a low-spin hexa-coordinated P450 heme (Fig. 2). The calculated K_d value for lauric acid was 27.5 ± 4.2 μM (Table 1). Similarly, capric acid and octanoic acid showed type I spectral changes, with K_d values 713 ± 46 μM and 144 ± 20 μM, respectively (Table 1). This result suggested that saturated fatty acids could be substrates for CYP6A8.

Table 1. Fatty acid binding affinities of CYP6A8

CYP6A8	K_d, μM		
	Octanoic acid	Capric acid	Lauric acid
	713 ± 46	144 ± 20	28 ± 4

Fatty acid hydroxylation of CYP6A8

The hydroxylation of lauric acid and capric acid catalyzed by CYP6A8 was analyzed using UPLC-MS/MS. Purified CYP6A8 converted lauric acid to two hydroxylated products eluting at 3.3 min and 3.4 min, in the SIR mode at m/z 215.3 (Fig. 3). The minor product was ω-hydroxylated lauric acid at 3.4 min and the major product was (ω-1)-hydroxylated lauric acid, as identified using co-chromatography with a standard hydroxylated compound and comparison with the reaction products from human CYP4A11 (Antoun *et al*., 2006). The steady-state kinetics of lauric acid hydroxylation was calculated. The kinetic parameters, that is, the k_{cat} and K_m values for (ω-1)-hydroxylation of lauric acid were 0.028 ± 0.002 min^{-1} and 10.1 ± 2.0 μM, respectively, and those for ω-hydroxylation were 0.009 ± 0.001 min^{-1} and 9.3 ± 2.8 μM, respectively (Fig. 4,

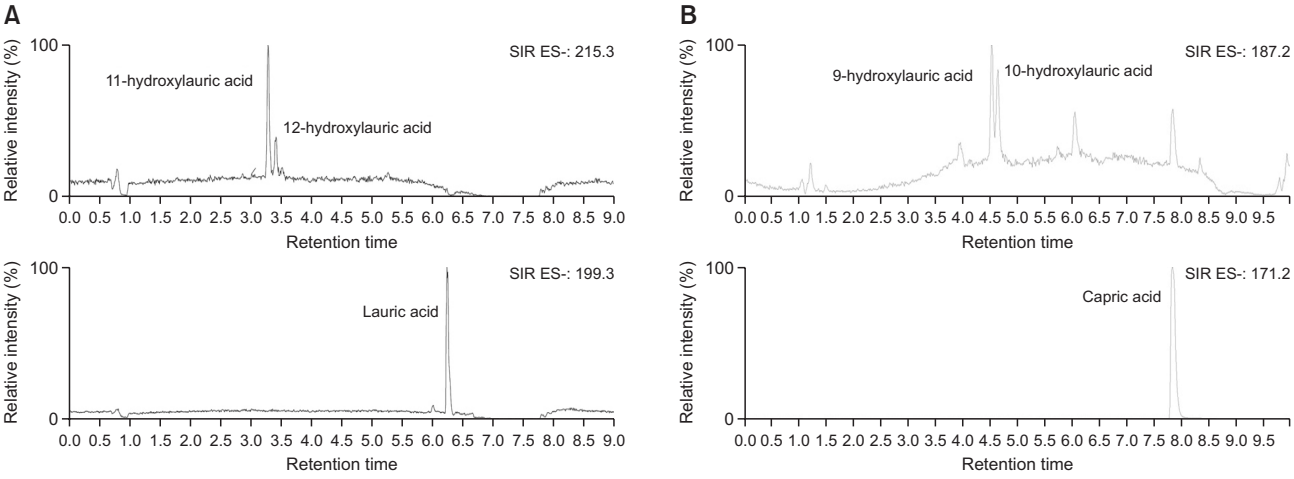

Fig. 3. Ultra-performance liquid chromatography (UPLC)-mass spectrometry chromatogram ω- and (ω-1)-hydroxylation of lauric and capric acid by purified CYP6A8 enzyme. (A) The retention time of lauric acid is 6.2 min, 11-hydroxylauric acid is 3.3 min, and 12-hydroxylauric acid is 3.4 min. (B) The retention time of capric acid is 7.8 min. The retention time of 9-hydroxycapric acid is 4.5 min and that of 10-hydroxycapric acid is 4.6 min.

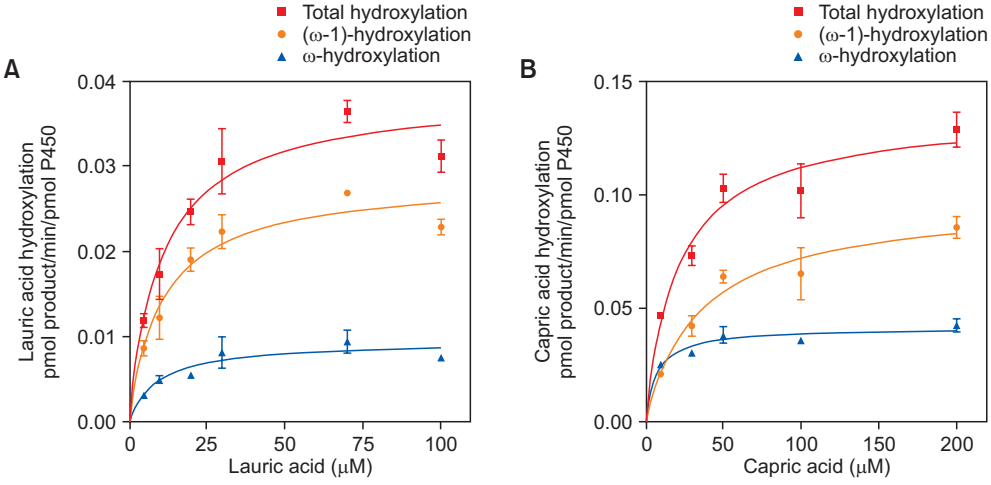

Fig. 4. Catalytic activity of purified CYP6A8 enzyme to lauric and capric acid. (A) Steady-state kinetic analysis of lauric acid ω-hydroxylation and (ω-1)-hydroxylation and total hydroxylation. (B) Steady-state kinetic analysis of capric acid ω-hydroxylation and (ω-1)-hydroxylation and total hydroxylation. Each point represents the mean ± SD (range) from triplicate assays. Steady-state kinetic parameters were obtained by fitting the values to a standard Michaelis–Menten equation using the GraphPad Prism software. The steady-state kinetic parameters are shown in Table 2.

Table 2). In the capric acid hydroxylation reaction catalyzed by CYP6A8, the (ω-1)-hydroxylated product was found to be the major metabolite (4.5 min) in the chromatogram in the SIR mode at m/z 187.26 (Fig. 3). A steady-state kinetic analysis of capric acid (ω-1)-hydroxylation yielded a k_{cat} value of 0.097 ± 0.007 min^{-1} and a K_m value of 35.0 ± 7.5 μM (Fig. 4, Table 2). The turn-over number for ω-hydroxylation of capric acid was lower than that of (ω-1)-hydroxylation with a k_{cat} of 0.042 ± 0.002 min^{-1}; however, the K_m value decreased to 7.1 ± 1.6 μM (Fig. 4, Table 2). These turn-over numbers of fatty acids hydroxylation by CYP6A8 are relatively lower than that of human CYP4A11 enzyme, which has been reported as 8.6 min (Kim *et al*., 2014).

DISCUSSION

In this study, the recombinant CYP6A8 enzyme from *D. melanogaster* displayed (ω-1)-hydroxylation of fatty acids, including lauric and capric acid. The binding spectrum analysis of the CYP6A8 enzyme to octanoic, capric, and lauric acids showed type I spectral changes, indicating that the active site architecture of this enzyme accommodates the productive substrate binding of many fatty acids with C8-C12. However, other longer saturated or unsaturated fatty acids, such as palmitic, stearic, oleic, arachidonic, and myristic acids, did not show any binding spectral titration for the CYP6A8 enzyme (data not shown). In addition, certain clinical drugs (bupropion, tolbutamide, and acetylsalicylic acid) and azole compounds (ketoconazole, econazole, miconazole, and clotrimazole) failed to display changes in their binding spectra for the CYP6A8 enzyme (data not shown). The calculated K_d value of octanoic acid was very high (Table 1), and no product was observed according to the UPLC-MS/MS analysis of the enzyme reaction (data not shown). We speculate that the length of the active access channel of CYP6A8 can only fit C10-C12 chained fatty acids to achieve the optimum orientation above the heme.

Rat NADPH-P450 reductase (NPR) was used as an electron redox partner for the purified CYP6A8 in the reconstituted P450 system. In a previous study on yeast microsome, a successful P450 catalytic reaction was achieved using *D. melanogaster* P450 reductase (DMR) (Helvig *et al*., 2004). Sequence alignment of rat, human, and fly P450 reductases showed very strong similarity in the putative P450 interaction domain, as well as FMN, FAD, and NADPH binding regions (Supplementary Fig. 1). The similarity score was 89.6%. The Arg at 246 in human and rat NPR was indicated as a key residue for electron transfer to P450 and was well conserved in fly reductase (Supplementary Fig. 1) (Campelo *et al*., 2017). Our results suggest that eukaryotic reductase can universally support any P450 system, including the *Drosophila* P450 enzyme. Our previous study showed that fungal NADPH-P450 reductase displayed successful transfer of electrons to the mammalian P450 system (Park *et al*., 2010, 2017).

In this study, CYP6A8 predominantly showed an oxidative catalysis reaction at the (ω-1)-position of the fatty acids rather than at the ω-position. Generally, fatty acid hydroxylase enzymes oxidize the terminal methyl group, which is thermodynamically disadvantageous compared to the methylene group (CaJacob *et al*., 1988). However, a specific ω-hydroxylation reaction of fatty acids was observed in certain P450 enzymes by presenting the terminal carbon of fatty acids to the heme iron through narrow channels, limiting access to other carbon atoms (Maitra *et al*., 1996; He *et al*., 2005; Kim *et al*, 2007). The active site architecture of P450 enzymes allows for the localization of fatty acid substrates in the form required for a

Table 2. Steady-state kinetic parameters of lauric acid and capric acid hydroxylation by CYP6A8

	Capric acid hydroxylation			Lauric acid hydroxylation		
	k_{cat}, min^{-1}	K_m, μM	k_{cat}/K_m, min^{-1} μM^{-1}	k_{cat}, min^{-1}	K_m, μM	k_{cat}/K_m, min^{-1} μM^{-1}
Total hydroxylation	0.135 ± 0.007	21.2 ± 4.2	0.0067 ± 0.0017	0.038 ± 0.002	10.7 ± 2.0	0.0038 ± 0.0009
(ω-1)-hydroxylation	0.097 ± 0.007	35.0 ± 7.5	0.0030 ± 0.0084	0.028 ± 0.002	10.1 ± 2.0	0.0028 ± 0.0007
ω-hydroxylation	0.042 ± 0.002	7.1 ± 1.6	0.0063 ± 0.0017	0.010 ± 0.001	9.3 ± 2.8	0.0012 ± 0.0005

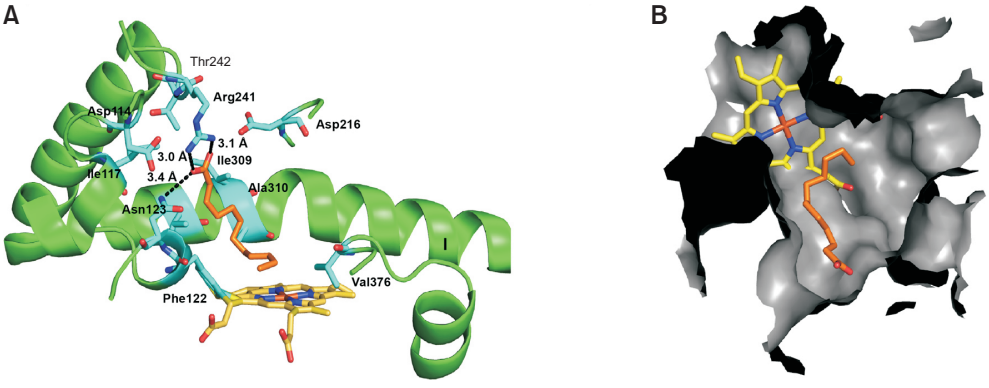

Fig. 5. Molecular docking models of CYP6A8. The molecular docking model was constructed using the SWISS-homology model structure of CYP6A8. (A) The amino acid residues interacting with lauric acid in the CYP6A8. The distance between the Arg241 residue of CYP6A8 and the hydrogen-bonded lauric acid was 3.0 Å and 3.1 Å, respectively. (B) The view of lauric acid in the active site space of CYP6A8.

particular reaction and exhibits regioselectivity through the active site structure (Hammerer *et al*., 2018). However, CYP6A8 appeared to possess a relatively large number of active sites. The estimated volume of the CYP6A8 active site obtained using CASTp and the USCF Chimera program was approximately 3764 Å^3. Additionally, the molecular model of CYP6A8 obtained using the SWISS MODEL program indicated that the active site appeared to be wide and not narrow or long (Fig. 5). This suggests that fatty acids in the active site could be obtained in a relatively flexible manner and that (ω-1)-hydroxylation could dominate without regioselectivity. Substrate docking modeling was performed using the AutoDockVina software, and the best docking model was selected on the basis of the heme-facing substrate for a productive reaction (Fig. 5A). The docking energy was –5.8 kcal/mol (RMSD of 7.553). In this docking model, the carboxyl group of lauric acid interacted with Arg residues and heme, with close distances of 3.0 Å and 3.1 Å, respectively; however, the overall molecule of lauric acid is flexible in a large active site (Fig. 5B).

The physiological role of CYP6A8 in the oxidation of fatty acids has not yet been established; however, many previous studies on insects have demonstrated that the oxidation of fatty acids plays an important role in the formation of pheromones in honeybees. The fatty acids of insects are converted to long-chain fatty aldehydes by acyl-CoA reductase; eventually, the CYP4G family catalyzes the production of hydrocarbons, which serve as cuticular waterproofing agents in insects (Plettner *et al*., 1997; Qiu *et al*., 2012; Miura, 2013). In addition, the locust *Locusta migratoria* ω-hydroxylase lauric acid in the fat body microsome (Feyereisen and Durst, 1980). Changes in the fatty acid content of insects can affect reproduction because they affect female fertility, reproductive performance, and sex hormone production (Fougeron *et al*., 2011). In mammals, CYP4A11 is an ω-hydroxylase that catalyzes lauric acid in the liver and kidney (Kim *et al*., 2014). This catalysis by CYP4A11 may reduce free fatty acid cellular accumulation and play an important role in maintaining membrane integrity (Adas *et al*., 1999). *D. melanogaster* may use P450 fatty acid hydroxylase enzymes for the similar role in the cellular membrane.

In conclusion, we overexpressed and purified CYP6A8 from *D. melanogaster* and performed a biochemical characterization. Characterization of the catalytic properties of this protein may provide a key to the P450-mediated reaction of various fatty acids in *D. melanogaster*. The physiological effects of fatty acids in *D. melanogaster* need to be determined in future studies, such as confirmation of the phenotype and generation of a mutant for determining the changed catalytic activity and studying the structure–function relationship of the P450 enzyme, including the role of the amino acid.

CONFLICT OF INTEREST

The authors declare that they have no conflicts of interest regarding the content of this article.

ACKNOWLEDGMENTS

This study was supported by an NRF grant, funded by the Korean government (NRF-2019R1A2C1004722).

REFERENCES

Adas, F., Salaün, J. P., Berthou, F., Picart, D., Simon, B. and Amet, Y. (1999) Requirement for ω and (ω–1)-hydroxylations of fatty acids by human cytochromes P450 2E1 and 4A11. *J. Lipid Res.* **40**, 1990-1997.

Amichot, M., Tarès, S., Brun-Barale, A., Arthaud, L., Bride, J. M. and Bergé, J. B. (2004) Point mutations associated with insecticide resistance in the *Drosophila* cytochrome P450 Cyp6a2 enable DDT metabolism. *Eur. J. Biochem.* **271**, 1250-1257.

Antoun, J., Amet, Y., Simon, B., Dréano, Y., Corlu, A., Corcos, L., Salaun, J. P. and Plée-Gautier, E. (2006) CYP4A11 is repressed by retinoic acid in human liver cells. *FEBS Lett.* **580**, 3361-3367.

CaJacob, C. A., Chan, W. K., Shephard, E. and Ortiz de Montellano, P. R. (1988) The catalytic site of rat hepatic lauric acid omega-hydroxylase. Protein versus prosthetic heme alkylation in the omega-hydroxylation of acetylenic fatty acids. *J. Biol. Chem.* **263**, 18640-18649.

Campelo, D., Lautier, T., Urban, P., Esteves, F., Bozonnet, S., Truan, G. and Kranendonk, M. (2017) The hinge segment of human NADPH-cytochrome P450 reductase in conformational switching: the critical role of ionic strength. *Front. Pharmacol.* **8**, 755.

Dunkov, B. C., Guzov, V. M., Mocelin, G., Shotkoski, F., Brun, A., Amichot, M., Ffrench-Constant, R. H. and Feyereisen, R. (1997) The Drosophila cytochrome P450 gene Cyp6a2: structure, localization, heterologous expression, and induction by phenobarbital. *DNA Cell Biol.* **16**, 1345-1356.

Feyereisen, R. (1999) Insect P450 enzymes. *Annu. Rev. Entomol.* **44**, 507-533.

Feyereisen, R. and Durst, F. (1980) Development of microsomal cytochrome P-450 monooxygenases during the last larval instar of the locust, Locusta migratoria: correlation with the hemolymph 20-hydroxyecdysone titer. *Mol. Cell. Endocrinol.* **20**, 157-169.

Fougeron, A. S., Farine, J. P., Flaven-Pouchon, J., Everaerts, C. and Ferveur, J. F. (2011) Fatty-acid preference changes during development in Drosophila melanogaster. *PLoS One* **6**, e26899.

Guengerich, F. P. (2018) Mechanisms of cytochrome P450-catalyzed oxidations. *ACS Catal.* **8**, 10964-10976.

Hammerer, L., Winkler, C. K. and Kroutil, W. (2018) Regioselective biocatalytic hydroxylation of fatty acids by cytochrome P450s. *Catal. Lett.* **148**, 787-812.

He, X., Cryle, M. J., De Voss, J. J. O. and de Montellano, P. R. (2005) Calibration of the channel that determines the omega-hydroxylation regiospecificity of cytochrome P4504A1: catalytic oxidation of 12-HALODOdecanoic acids. *J. Biol. Chem.* **280**, 22697-22705.

Helvig, C., Tijet, N., Feyereisen, R., Walker, F. A. and Restifo, L. L. (2004) Drosophila melanogaster CYP6A8, an insect P450 that catalyzes lauric acid (omega-1)-hydroxylation. *Biochem. Biophys. Res. Commun.* **325**, 1495-1502.

Kim, D., Cha, G.-S., Nagy, L. D., Yun, C.-H. and Guengerich, F. P. (2014) Kinetic analysis of lauric acid hydroxylation by human cytochrome P450 4A11. *Biochemistry* **53**, 6161-6172.

Kim, D., Cryle, M. J., De Voss, J. J. and Ortiz de Montellano, P. R. (2007) Functional expression and characterization of cytochrome P450 52A21 from Candida albicans. *Arch. Biochem. Biophys.* **464**, 213-220.

Maitra, S., Dombrowski, S. M., Waters, L. C. and Ganguly, R. (1996) Three second chromosome-linked clustered Cyp6 genes show differential constitutive and barbital-induced expression in DDT-resistant and susceptible strains of Drosophila melanogaster. *Gene* **180**, 165-171.

Miura, Y. (2013) The biological significance of ω-oxidation of fatty acids. *Proc. Jpn. Acad. Ser. B* **89**, 370-382.

Niwa, R., Matsuda, T., Yoshiyama, T., Namiki, T., Mita, K., Fujimoto, Y. and Kataoka, H. (2004) CYP306A1, a cytochrome P450 enzyme, is essential for ecdysteroid biosynthesis in the prothoracic glands of Bombyx and Drosophila. *J. Biol. Chem.* **279**, 35942-35949.

Park, H. G., Lim, Y. R., Eun, C. Y., Han, S., Han, J. S., Cho, K. S., Chun, Y. J. and Kim, D. (2010) Candida albicans NADPH-P450 reductase: expression, purification, and characterization of recombinant protein. *Biochem. Biophys. Res. Commun.* **396**, 534-538.

Park, H. G., Lim, Y. R., Han, S., Jeong, D. and Kim, D. (2017) En-

hanced purification of recombinant rat NADPH-P450 reductase by using a hexahistidine-tag. *J. Microbiol. Biotechnol.* **27**, 983-989.

Plettner, E., Otis, G. W., Wimalaratne, P. D. C., Winston, M. L., Slessor, K. N., Pankiw, T. and Punchihewa, P. W. K. (1997) Species- and caste-determined mandibular gland signals in honeybees (Apis). *J. Chem. Ecol.* **23**, 363-377.

Pondeville, E., David, J. P., Guittard, E., Maria, A., Jacques, J. C., Ranson, H., Bourgouin, C. and Dauphin-Villemant, C. (2013) Microarray and RNAi analysis of P450s in Anopheles gambiae male and female steroidogenic tissues: CYP307A1 is required for ecdysteroid synthesis. *PLoS One* **8**, e79861.

Qiu, Y., Tittiger, C., Wicker-Thomas, C., Le Goff, G., Young, S., Wajnberg, E., Fricaux, T., Taquet, N., Blomquist, G. J. and Feyereisen, R. (2012) An insect-specific P450 oxidative decarbonylase for cuticular hydrocarbon biosynthesis. *Proc. Natl. Acad. Sci. U.S.A.* **109**, 14858-14863.

Seong, K. M., Coates, B. S., Berenbaum, M. R., Clark, J. M. and Pittendrigh, B. R. (2018) Comparative CYP-omic analysis between the DDT-susceptible and -resistant Drosophila melanogaster strains 91-C and 91-R. *Pest Manage. Sci.* **74**, 2530-2543.

Tijet, N., Helvig, C. and Feyereisen, R. (2001) The cytochrome P450 gene superfamily in Drosophila melanogaster: annotation, intron-exon organization and phylogeny. *Gene* **262**, 189-198.

Wang, L., Dankert, H., Perona, P. and Anderson, D. J. (2008) A common genetic target for environmental and heritable influences on aggressiveness in Drosophila. *Proc. Natl. Acad. Sci. U.S.A.* **105**, 5657.

Werck-Reichhart, D. and Feyereisen, R. (2000) Cytochromes P450: a success story. *Genome Biol.* **1**, reviews3003.1.